

Metadata of the chapter that will be visualized in SpringerLink

Book Title	Computational Intelligence and Optimization Methods for Control Engineering	
Series Title		
Chapter Title	A Real-Time Big Data Control-Theoretical Framework for Cyber-Physical-Human Systems	
Copyright Year	2019	
Copyright HolderName	Springer Nature Switzerland AG	
Corresponding Author	Family Name Particle Given Name Prefix Suffix Role Division Organization Address Email	Gusrialdi Azwirman Xu Ying Qu Zhihua Simaan Marwan A.
Author	Family Name Particle Given Name Prefix Suffix Role Division Organization Address Email	University of Central Florida Orlando, 32816, USA azwirman.gusrialdi@ucf.edu
Author	Family Name Particle Given Name Prefix Suffix Role Division Organization Address Email	University of Central Florida Orlando, 32816, USA ying.xu@ucf.edu
Author	Family Name Particle Given Name Prefix Suffix Role Division Organization Address Email	University of Central Florida Orlando, 32816, USA qu@ucf.edu
Author	Family Name Particle Given Name Prefix Suffix	

Role
Division
Organization University of Central Florida
Address Orlando, 32816, USA
Email simaan@eeecs.ucf.edu

Abstract

Cyber-physical-human systems naturally arise from interdependent infrastructure systems and smart connected communities. Such applications require ubiquitous information sensing and processing, intelligent machine-to-machine communication for a seamless coordination, as well as intelligent interactions between humans and machines. This chapter presents a control-theoretical framework to model heterogeneous physical dynamic systems, information and communication, as well as cooperative controls and/or distributed optimization of such interconnected systems. It is shown that efficient analytical and computational algorithms can be modularly designed and hierarchically implemented to operate and optimize cyber-physical-human systems, first to quantify individually the input–output relationship of nonlinear dynamic behaviors of every physical subsystem, then to coordinate locally both cyber-physical interactions of neighboring agents as well as physical-human interactions, and finally to dynamically model and optimize the overall networked system. The hierarchical structure makes the overall optimization and control problem scalable and solvable. Moreover, the three levels integrate individual designs and optimization, distributed cooperative optimization, and decision-making through real-time, data-driven, model-based learning and control. Specifically, one of the contributions of the chapter is to demonstrate how the combination of dissipativity theory and cooperative control serves as a natural framework and promising tools to analyze, optimize, and control such large-scale system. Application to digital grid is investigated as an illustrative example.

Chapter 7

A Real-Time Big Data Control-Theoretical Framework for Cyber-Physical-Human Systems



Azwirman Gusrialdi, Ying Xu, Zhihua Qu and Marwan A. Simaan

1 **Abstract** Cyber-physical-human systems naturally arise from interdependent infrastructure systems and smart connected communities. Such applications require ubiquitous information sensing and processing, intelligent machine-to-machine communication for a seamless coordination, as well as intelligent interactions between humans and machines. This chapter presents a control-theoretical framework to model heterogeneous physical dynamic systems, information and communication, as well as cooperative controls and/or distributed optimization of such interconnected systems. It is shown that efficient analytical and computational algorithms can be modularly designed and hierarchically implemented to operate and optimize cyber-physical-human systems, first to quantify individually the input–output relationship of non-linear dynamic behaviors of every physical subsystem, then to coordinate locally both cyber-physical interactions of neighboring agents as well as physical-human interactions, and finally to dynamically model and optimize the overall networked system. The hierarchical structure makes the overall optimization and control problem scalable and solvable. Moreover, the three levels integrate individual designs and optimization, distributed cooperative optimization, and decision-making through real-time, data-driven, model-based learning and control. Specifically, one of the contributions of the chapter is to demonstrate how the combination of dissipativity theory and cooperative control serves as a natural framework and promising tools to analyze, optimize, and control such large-scale system. Application to digital grid is investigated as an illustrative example.

A. Gusrialdi (✉) · Y. Xu · Z. Qu · M. A. Simaan
University of Central Florida, Orlando 32816, USA
e-mail: azwirman.gusrialdi@ucf.edu

Y. Xu
e-mail: ying.xu@ucf.edu

Z. Qu
e-mail: qu@ucf.edu

M. A. Simaan
e-mail: simaan@eecs.ucf.edu

© Springer Nature Switzerland AG 2019
M. J. Blondin et al. (eds.), *Computational Intelligence and Optimization Methods for Control Engineering*, Springer Optimization and Its Applications 150,
https://doi.org/10.1007/978-3-030-25446-9_7

22 7.1 Introduction

AQ1 23 Cyber-physical-systems (CPSs) refer to the integrations of cyber core consisting of
AQ2 24 communication network, computation and physical processes (engineered systems)
25 which are normally large scale and complex, as illustrated in Fig. 7.1. These two
26 components are tightly coupled: embedded computers and networks monitor and
27 control the physical processes, usually with feedback loops where physical pro-
28 cesses affect computations and vice versa. In addition, CPSs will also interact with
29 humans resulting in cyber-physical-human systems. Cyber-physical-human systems
30 naturally arise from interdependent infrastructure systems and smart connected com-
31 munities. Examples include smart grid [54], intelligent transportation systems [16],
32 and smart city [5]. Such applications require ubiquitous information sensing and pro-
33 cessing, intelligent machine-to-machine communication, a seamless coordination of
34 physical systems, and intelligent interactions between humans and machines. While
AQ3 35 technological advances and the development of relatively inexpensive yet power-
36 ful communication, computation, and sensing devices make the realization of such
37 complex system feasible, fundamental technical challenges centered on real-time big
38 data processing, optimization, and control of the spatially distributed complex sys-
39 tems remain to be solved. A major and fundamental challenge is to develop a control
40 design theory that does not consider the physical and cyber components separately,
41 but as two facets of the same system [2]. Another major challenge is the choice of
42 control architecture which allows the designer to control the complex system effi-
43 ciently and in real time. Traditional centralized control architecture, where all the
44 data from ubiquitous sensors are gathered in a centralized processing center, which
45 optimizes and computes the control input for the overall system is not appropriate to
46 optimize and control such large-scale interconnected system since it may suffer from
47 explosion of data and may also harm data privacy [4]. This calls for a scalable and
48 modular system theoretic tools to analyze, optimize, and control the cyber-physical-
49 human systems. In particular, distributed optimization and control algorithms are
50 highly desirable for dealing with such complex systems due to its scalability and
51 robustness against component faults and cyberattacks [17].

52 The chapter presents a control-theoretical framework to model heterogeneous
53 physical dynamic systems, information and communication, as well as cooperative
54 controls and/or distributed optimization through which human operator or users can
55 interact effectively with physical systems in a multi-agent setting to achieve various
56 control and optimization objectives. It is shown that efficient computational algo-
57 rithms can be applied hierarchically to operate and optimize cyber-physical-human
58 systems, first individually to quantify the dynamic behavior of every agent, then
59 locally to describe the local interactions of neighboring agents, and finally to the
60 overall system. All the three control levels deal with real-time big data, and the
61 hierarchical structure makes the overall optimization and control problem scalable
62 and solvable. In particular, one of the contributions is to demonstrate how the con-
cept of dissipativity theory and cooperative control serve as a natural framework

and promising tools to analyze, optimize, and control such large-scale systems in a scalable and modular manner. Application to digital power grid is investigated as an illustrative example.

The chapter is organized as follows. We begin with dynamic modeling of cyber-physical-human systems together with its optimization and control objectives in Section 7.2. A brief summary of the basic concepts of dissipativity theory and cooperative control as the main analytical and design tools is presented in Section 7.3. Section 7.4 provides an example of applying the dissipativity theory and cooperative control to design hierarchical control of power system. Modeling and analysis of human-machine interaction with focus on electricity market are presented in Section 7.5. The role of real-time big data and decision-making in controlling cyber-physical-human systems is discussed in Section 7.6. Finally, we conclude in Section 7.7.

7.2 Dynamic Modeling of Cyber-Physical Systems and Its Optimization/Control Objectives

System modeling is an important step in designing control algorithms. Briefly speaking, a model is a mathematical representation of physical system which allows us to reason and predict how the system will behave. In this chapter, we are mainly interested in models of dynamical system describing the input/output behavior of systems. To this end, let us consider cyber-physical-human systems consisting of n heterogeneous physical systems whose individual dynamics can be modeled by differential equations in the form of

$$\dot{x}_i = f_i(x_i, u_i, r_i), \quad y_i = h_i(x_i, r_i), \quad (7.1)$$

with $i = \{1, \dots, n\}$. The model in (7.1) is known as state-space models where variables $x_i \in \Re^{n_i}$ denote the state which encodes what needs to be known about the past history, $u_i \in \Re^m$ is the control signals to be designed, and $y_i \in \Re^m$ denotes the output (measurement) signals of the i -th system. In addition, $r_i \in \Re^m$ in (7.1) is the operational decision as a result of the intelligent interaction between humans and the physical systems which may take place in a slower timescale. In general, the physical systems may also be interconnected through a physical network whose characteristic could be described by the following algebraic equation:

$$\kappa_i(y_1, \dots, y_n, x_1, \dots, x_n) = 0. \quad (7.2)$$

As an example, consider a power system where the individual physical system refers to the synchronous generator as shown in Fig. 7.1. For the sake of simplicity, the dynamics of synchronous generator is given by the following swing equation:

$$M_i \ddot{\delta}_i = P_{m,i} - P_{e,i} - D_i \omega_0 \dot{\delta}_i, \quad (7.3)$$

99 where $M_i > 0$ denotes its inertia, $D_i > 0$ is its damping constant, $P_{m,i}$ denotes its
100 mechanical power while $P_{e,i}$ is its active power output, and δ_i denotes its rotor
101 angle measured with respect to a rotating frame with speed ω_0 . The generators are
102 physically interconnected with each other which can be characterized through the
103 following nonlinear power flow equation:

$$104 \quad P_{e,i} = E_i^2 G_{ii} + \sum_{k \neq i} E_i E_k (G_{ik} \cos \delta_{ik} + B_{ik} \sin \delta_{ik}), \quad (7.4)$$

105 where $\delta_{ik} = \delta_i - \delta_k$, E_i is the voltage of the generator bus, and $Y_{ik} = G_{ik} + j B_{ik}$
106 is the transfer admittance between generators i and k . Defining, respectively, the
107 states, input and output of the i -th generator as $x_i = [\delta_i - \delta_i^*, \omega_i]^T$, $u_i = P_{m,i}$ and
108 $y_i = x_i$ with δ_i^* denotes the final angle, we can recast swing equation (7.3) together
109 with power flow equation (7.4) with respect to their equilibrium in the form of (7.1)
110 as [22]

$$111 \quad \dot{x}_i = A_i(x_i)x_i + B_i(x_i)u_i + \sum_{k \in \mathcal{N}_i} H_{ik}(y_i, y_k)(y_k - y_i), \quad y_i = C_i x_i, \quad (7.5)$$

112 where \mathcal{N}_i denotes the neighboring set of generator i , matrices A_i , B_i and coupling
113 matrix H_{ik} are state/output-dependent. Note that generators with higher (e.g., fifth
114 or sixth) order dynamics can also be represented by state-space model (7.5). In
115 addition to the physical network, there is also a cyber-layer representing informa-
116 tion/communication network for the system operator/local controller of physical
117 systems to obtain/exchange measurements in order to monitor and control the over-
118 all system. The structure of communication network (information flow) in general is
119 modeled using a graph as illustrated in Fig. 7.1. Let \mathcal{N}_i^c denote the communication
120 neighboring set of the i -th subsystem. In other words, subsystem $j \in \mathcal{N}_i^c$ if infor-
121 mation on measurement y_j is available to the i -th subsystem. The communication
122 network topology can also be represented by the following communication matrix:

$$123 \quad S^c = [S_{ij}^c] \in \mathbb{R}^{n \times n}, \quad S_{ii}^c = 1, \quad (7.6)$$

124 where $S_{ij}^c = 1$ if $j \in \mathcal{N}_i^c$ and $S_{ij}^c = 0$ otherwise.

125 Optimizing and controlling the above cyber-physical-human systems calls for
126 computationally efficient and scalable algorithms to deal with its large-scale nature
127 and complexity (in terms of heterogeneous individual nonlinear dynamics and their
128 physical interconnections). To this end, we divide the control objective of cyber-
129 physical-human systems into three levels as illustrated in Fig. 7.2. Specifically, the
130 control input u_i in (7.1) is decomposed into the following hierarchical form:

$$131 \quad u_i = u_{s_i}(x_i) + \underbrace{u_{l_i}(y_i, y_j) + v_i}_{\bar{u}_i}, \quad (7.7)$$

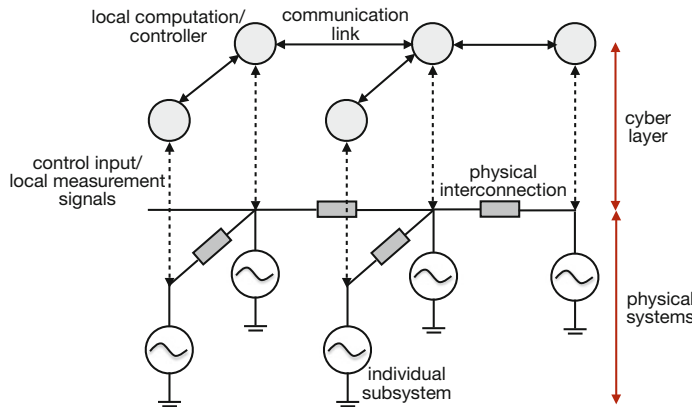


Fig. 7.1 An illustrative diagram of cyber-physical systems as exemplified by power system

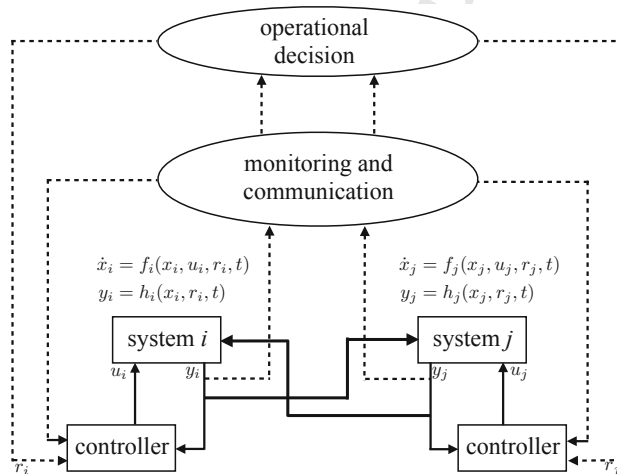


Fig. 7.2 Three-level data-driven controls of cyber-physical-human systems. The dashed lines represent information flow between different levels

132 each layer with the following control design objective:

133 1. the lowest level control u_{s_i} aims to stabilize each individual physical system,
 134 2. the mid-level control input u_{l_i} is to achieve a local coordination for a group of
 135 physical systems, and
 136 3. the highest level control v_i aims at ensuring stability of the overall interconnected
 137 system.

138 For the example of power system whose dynamics is represented by (7.5), the goal
 139 of low-level (self-feedback) control u_{s_i} is to ensure (input–output) stability of the
 140 individual generator. The mid-level control u_{l_i} can be designed as a distributed opti-

141 mization algorithm (by taking advantage of the communication network) to achieve
 142 a uniform voltage profile for a group of generators or minimize power loss. Finally,
 143 the high-level control v_i acts as a wide-area control with the goal of ensuring stability
 144 and/or improving performance of the power system.

145 In what follows, we will present a control theoretic framework based on dissipativity
 146 theory and cooperative control for systematically optimizing and controlling
 147 cyber-physical-human systems and further demonstrate its effectiveness using the
 148 power system example described previously.

149 7.3 Main Analytical and Design Tools: Dissipativity 150 Theory and Cooperative Control

151 Dissipativity is an energy-like concept which describes input–output properties (e.g.,
 152 stability) of a dynamical system. Input–output mapping becomes a useful way of
 153 quantifying input–output properties of the system when the dynamical model of the
 154 system is not available. Briefly speaking, dissipative system is a system that absorbs
 155 more energy from the external world than it supplies [23]. Passivity is a special
 156 class of dissipativity and is originated in circuit analysis. Passive systems are always
 157 decreasing in energy with respect to input energy. For example, an electrical circuit
 158 consisting of resistor, inductor, and capacitor can dissipate energy by turning it into
 159 heat and also store energy, but it cannot supply more energy than what has been put
 160 into it. Another class of dissipative systems is what so-called passivity-short systems.
 161 Compared to passive systems, passivity-short systems may increase or remain the
 162 same in energy from input to output during transience. One example is a generator
 163 that is not decreasing in energy at all times simply because it is producing some
 164 amount of energy. Dissipativity-based approaches become attractive in analyzing
 165 and controlling CPS since its properties are preserved over system interconnections
 166 which makes the approach computationally scalable. For example, with individual
 167 output negative feedback, the passivity-short systems can be interconnected either in
 168 parallel or in series or in a positive feedback loop or a negative feedback loop while
 169 maintaining the same passivity-short property [21]. This compositional property
 170 makes dissipativity a powerful and promising tool to analyze and control large-scale
 171 system such as CPS [2].

172 The concept of dissipativity is captured by introducing two energy-like functions,
 173 namely, supply rate and storage functions. Depending on the choice of particular
 174 supply rate function, dissipativity can imply several important behaviors such as
 175 stability of dynamical systems and their interconnections. Consider system (7.1)
 176 with $r_i = 0$ and without physical interconnection. The i -th system with supply
 177 rate $\Phi_i(u_i(t), y_i(t))$ is said to be dissipative if there exists a nonnegative real storage
 178 function $V_i(x_i)$ such that the following inequality holds [45]:

$$179 V_i(x_i(t)) - V_i(x_i(0)) \leq \int_0^t \Phi_i(u_i(\tau), y_i(\tau)) d\tau. \quad (7.8)$$

180 Choosing the supply rate function in a quadratic form, the i -th system is said to be
 181 input passivity-short with respect to a differentiable storage function $V_i(x_i)$ if the
 182 inequality

$$183 \quad \dot{V}_i \leq u_i^T y_i + \frac{\varepsilon_{ii}}{2} \|u_i\|^2 - \frac{\rho_i}{2} \|y_i\|^2 \quad (7.9)$$

184 holds for some $\varepsilon_{ii} > 0$, $\rho_i \geq 0$, and it is said to be output passivity-short if (7.9)
 185 holds for some $\varepsilon_{ii} \leq 0$, $\rho < 0$. In addition, the system is said to be L_2 stable if
 186 inequality (7.9) holds for some $\rho_i > 0$ and a positive definite V_i resulting in

$$187 \quad \|y_i\|_{L_2} \leq \left(\frac{2\varepsilon_{ii}}{\rho_i} + \frac{4}{\rho_i^2} \right) \|u_i\|_{L_2} + \text{constant.} \quad (7.10)$$

188 Finally, the system is passive if inequality (7.9) holds for some $\varepsilon_{ii} = 0$ (and $\rho_i = 0$).
 189 Figure 7.3 illustrates a static input–output mapping of passivity and passivity-short
 190 systems. Note that passivity is quite restricted as it excludes most of linear dynamic
 191 systems such as nonminimum-phase systems and minimum-phase systems with rela-
 192 tive degree 2 or higher. It is shown in [27] that most linear systems are passivity-short
 193 and that all linear Lyapunov-stable dynamic systems are either passivity-short or can
 194 be made passivity-short under an output-feedback control. The parameters ε_{ii} and ρ_i
 195 are important for analysis, control design, and stability of networked passivity-short
 196 systems, and it is desirable to maximize the value of ρ_i and minimize ε_{ii} . In par-
 197 ticular, ε_{ii} is also called *impact coefficient* and it quantifies the impact of individual
 198 passivity-short system on the network-level cooperative control as will be discussed
 199 later. Let us show now that a synchronous generator connected to infinite bus is
 200 passivity-short. Dynamics of the generator is given by the following swing equation:

$$201 \quad M_i \ddot{\delta}_i = b_i u_i - H_{ii}(\delta_i - \delta_i^*) - D_i \omega_0 \dot{\delta}_i \quad (7.11)$$

202 and its output is defined as $y_i \triangleq \delta_i - \delta_i^*$. Taking the following positive definite storage
 203 function:

$$204 \quad V_i = \left(\frac{k_d}{2k\sqrt{kp}} + \frac{\sqrt{kp}}{kk_d} \right) y_i^2 + \frac{1}{kk_d\sqrt{kp}} \dot{y}_i^2 + \frac{1}{k\sqrt{kp}} y_i \dot{y}_i$$

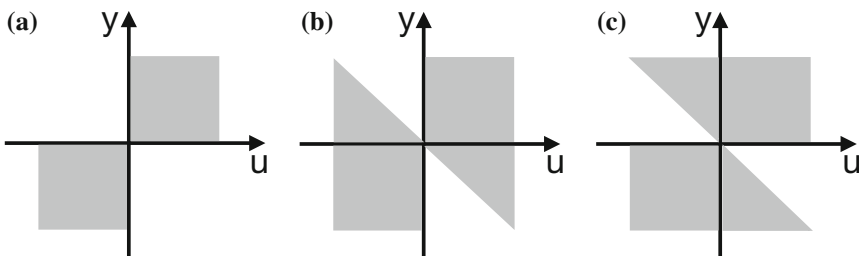


Fig. 7.3 Input–output diagram (shaded region) [22] of: a passive; b input passivity-short; c output passivity-short

205 with $k = b_i/M_i$, $k_p = H_{ii}/M_i$, and $k_d = D_i\omega_0/M_i$ and computing its derivative
206 yields

207
$$\dot{V}_i \leq u_i^T y_i + k \left(\frac{(1 - \sqrt{k_p})^2}{2k_p \sqrt{k_p}} + \frac{1}{k_d^2 \sqrt{k_p}} \right) u_i^2 - \frac{\sqrt{k_p}}{2k} y_i^2 \triangleq u_i^T y_i + \frac{\varepsilon_i}{2} \|u_i\|^2 - \frac{\rho_i}{2} \|y_i\|^2$$

208 which shows that the generator is passivity-short and L_2 stable. Furthermore, we
209 can also obtain the physical meanings of ε_i and ρ_i . To this end, the transfer function
210 of (7.11) can be written as

211
$$G(s) = \frac{k}{s^2 + k_d s + k_p}. \quad (7.12)$$

212 By writing $k_d = 2\xi\omega_n$, $k_p = \omega_n^2$, and $k \approx k_p$ where ω_n is the natural frequency and ξ
213 denotes the damping ratio, it can be shown that

214
$$\varepsilon_i \approx \omega_n \left(1 - \frac{1}{\omega_n} \right)^2 + \frac{1}{2\xi^2\omega_n}, \quad \rho_i \approx \frac{1}{\omega_n}.$$

215 Hence, we can see that the value of ε_i increases as ξ becomes smaller and the optimal
216 value of ε_i is obtained for $\omega_n = 1$.

217 Cooperative control is another control design tool that has shown a great promise
218 in optimizing and controlling large-scale system and has been successfully utilized to
219 develop network-level control of a group of mobile robots [3, 18], power system [54],
220 charging scheduling of electric vehicles [16], and complex network [15]. The goal of
221 cooperative control is to achieve nontrivial consensus using only local information
222 (and thus scalable) obtained via the communication network as illustrated in Fig. 7.1,
223 that is for all individual systems i , we have [42]

224
$$\lim_{t \rightarrow \infty} \|y_i(t) - y_j(t)\| = 0, \text{ or } \lim_{t \rightarrow \infty} y_i(t) = c. \quad (7.13)$$

225 Consider again physically decoupled CPS with individual dynamics (7.1). As shown
226 in [44], the concept of passivity-short simplifies the design of cooperative control
227 by modularizing the lower level and network-level control designs. Specifically, a
228 self-feedback control u_{s_i} is first designed so that individual system becomes passivity-
229 short. The cooperative control can then be designed by simply considering the fol-
230 lowing fictitious integrator dynamics:

231
$$\dot{y}_i = u_{l_i} \quad (7.14)$$

232 where u_{l_i} is specified as

233
$$u_{l_i} = k_{y_i} \sum_{j \in \mathcal{N}_i^c} S_{ij}^c (y_j - y_i). \quad (7.15)$$

234 The closed-loop dynamics of (7.14) and (7.15) can be compactly written as

235
$$\dot{y} = -\text{diag}\{k_{y_1}, \dots, k_{y_n}\}Ly, \quad (7.16)$$

236 with $y = [y_1, \dots, y_n]^T$ and $L = \text{diag}\{S^c \mathbb{1}\} - S^c$. Consensus (7.13) is ensured if
 237 there is at least one node from which every other node can be reached and the
 238 gains $k_{y_i} > 0$ are chosen to be smaller than k^* . Moreover, if every node can be
 239 reached from any other nodes, k^* can then be computed according to [44]

240
$$k^* = \frac{\lambda_2(\Gamma L + L^T \Gamma)}{2(\max_i \varepsilon_{ii})\lambda_{\max}(L^T \Gamma L)}, \quad (7.17)$$

241 where $\lambda_2(\cdot)$, $\lambda_{\max}(\cdot)$ denote the smallest nonzero and largest eigenvalues, respec-
 242 tively, and matrix $\Gamma = \text{diag}\{\eta_1\}$ with $\eta_1^T L = 0$. It is worth to note that k^* in (7.17) can
 243 be computed in a distributed manner without requiring global information of L [12].
 244 The communication topology embedded in matrix L can also be optimized to increase
 245 the convergence speed of (7.15), see, e.g., [9, 11, 43]. As can be seen from (7.15)
 246 and (7.17), the design of cooperative control of networked passivity-short system
 247 does not require any explicit knowledge about the heterogeneous physical systems
 248 other than their impact coefficients. Moreover, quantity $\max_i \varepsilon_{ii}$ in (7.17) can be
 249 viewed as the “worst” value of impact coefficients of all the passivity-short systems.
 250 Adding or removing subsystems into or from the networked systems results in differ-
 251 ent impacts on the overall system operation. However, the performance of the overall
 252 system can still be guaranteed given that the control gains are appropriately upper
 253 bounded to limit such impact. Hence, the operation of the networked system can be
 254 performed in a plug-and-play manner while its stability is guaranteed.

255 **7.4 Hierarchical Control Design for**
 256 **Cyber-Physical-Human Systems**

257 In this section, we utilize the concept of passivity-short and cooperative control
 258 presented in the previous section to design hierarchical control law (7.7) for power
 259 system whose dynamics is given by (7.5).

260 **7.4.1 Low-Level Control Design: Ensuring Input–Output**
 261 **Stability**

262 Let us now consider the nominal subsystem in (7.5) by excluding its physical inter-
 263 connections, i.e., assuming $H_{ik} = 0$ for all $i \neq k$. The first step is to design a self-
 264 feedback control u_{s_i} for individual physical system given by

265 $u_{s_i} = -K_i x_i$

266 such that (i) the individual physical system is passivity-short and L_2 stable for input–
 267 output pair $\{\bar{u}_i, y_i\}$; (ii) its impact on the overall system, that is, the values ε_{ii} and $-\rho_i$
 268 in (7.9) are minimized. To this end, taking the storage function $V = \frac{1}{2}x_i^T P_i x_i$ with
 269 P_i is a positive definite matrix, a self-feedback control can be designed by solving
 270 the following optimization problem:

$$\begin{aligned} & \underset{K_i, \varepsilon_{ii}, \rho_i}{\text{minimize}} \quad [\alpha_{ii} \varepsilon_{ii} - (1 - \alpha_{ii} \rho_i)] \\ & \text{subject to} \quad P_i > 0, \\ & \quad M_i(x_i) \leq 0, \\ & \quad \varepsilon_{ii}, \rho_i \geq 0, \end{aligned} \quad (7.18)$$

272 where $\alpha_{ii} \in (0, 1)$ is a design parameter and matrix $M_i(x_i)$ is defined as

273
$$M_i(x_i) \triangleq (A_i(x_i) - B_i K_i)^T P_i + P_i (A_i(x_i) - B_i K_i) + \rho_i C_i^T C_i + \frac{1}{\varepsilon_{ii}} \|P_i B_i - C_i^T\|^2 < 0.$$

274 The second constraint in (7.18) guarantees that inequality (7.9) holds, i.e., the individual system is passivity-short and L_2 stable. Note that at any instant of time t ,
 275 the state $x_i(t)$ becomes known from the Phasor Measurement Units (PMU) and so is
 276 matrix $A_i(x_i)$, and hence K_i can be designed adaptively by using available Lyapunov
 277 function $P_i > 0$.

279 After making the individual system passivity-short and L_2 stable, next we consider
 280 the interconnected system to quantify the impact of nonlinear interconnections on
 281 subsystem (7.5) in a way parallel to that of $\varepsilon_{ii} \|\bar{u}_i\|^2$. Specifically, the goal is to
 282 minimize the transient impacts of the inter-area oscillations encoded in ε_{ij} by solving
 283 the following optimization problem:

$$\begin{aligned} & \underset{\varepsilon_{ij}}{\text{minimize}} \quad \sum_{j \in \mathcal{N}_i} \alpha_{ij} \varepsilon_{ij} \\ & \text{subject to} \quad P_i > 0, \\ & \quad M'_i(x_i, y_j) \leq 0, \\ & \quad \varepsilon_{ij}, \alpha_{ij} \geq 0, \\ & \quad \sum_{j \in \mathcal{N}_i} \alpha_{ij} = 1, \end{aligned} \quad (7.19)$$

285 where

286
$$M'_i \triangleq M_i - \sum_{j \in \mathcal{N}_i} \left(P_i H_{ij} C_i + C_i^T H_{ij}^T P_i - \frac{1}{\varepsilon_{ij} P_i H_{ij} H_{ij}^T P_i} \right).$$

287 The second constraint in (7.19) guarantees that the following property holds:

288

$$\dot{V}_i \leq \bar{u}_i^T y_i + \frac{\varepsilon_{ii}}{2} \|\bar{u}_i\|^2 - \frac{\rho_i}{2} \|y_i\|^2 + \frac{1}{2} \sum_{j \in \mathcal{N}_i} \varepsilon_{ij} \|y_j\|^2,$$

289 where the terms $\varepsilon_{ij} \|y_j\|^2$ quantify the impact of nonlinear interconnections on the
290 subsystem. Standard techniques to solve Linear or Bilinear Matrix Inequality [51]
291 can be readily used to compute the solutions to both optimization problems (7.18)
292 and (7.19).

293 **7.4.2 Mid-level Control Design: Local Coordination Through
294 Cyber-Physical Interconnection**

295 Next, we design local coordination (cooperative) control u_{l_i} in (7.7) to improve the
296 voltage profile of the power system. As a scenario, we consider a distribution network
297 divided into several clusters as illustrated in Fig. 7.5. The goal is for the distributed
298 generators (DGs) to cooperatively control their reactive power injection such that
299 the sum of quadratic voltage errors of the DGs in each cluster is minimized. The
300 problem can be formulated as the following optimization problem:

301

$$\min_{\vartheta_i} \sum_i f_i, \quad f_i = \frac{1}{2} (1 - E_i)^2, \quad (7.20)$$

302 where the control variable are DGs reactive power fair utilization ratios ϑ_i defined
303 as $\vartheta_i = Q_{e_i} / \bar{Q}_{e_i}$ with \bar{Q}_{e_i} denotes the maximum reactive power available to the i -th
304 DG. The reactive power and voltage are coupled through the following power flow
305 equation:

306

$$Q_{e_i} = -E_i^2 B_{ii} + \sum_{k \neq i} E_i E_k (G_{ik} \sin \delta_{ik} - B_{ik} \cos \delta_{ik}).$$

307 In addition, it is also desirable for the DGs in each cluster to contribute equally (i.e.,
308 the values ϑ_i reach a consensus for all DGs) in minimizing (7.20). To this end, the
309 communication network is assumed to be bidirectional whose topology is similar to
310 that of the distribution network as shown in Fig. 7.4. Cooperative control algorithm
311 can then be designed to solve (7.20) as described in Section 7.3. Specifically, each
312 DG adjusts its reactive power fair utilization ratio according to

313

$$\dot{\vartheta}_i = u_{l_i} = \sum_{j \in \mathcal{N}_i^c} (\vartheta_j - \vartheta_i) - \beta_i \frac{\partial f_i}{\partial \vartheta_i}, \quad (7.21)$$

314 where $\beta_i > 0$ [33]. The first term of update rule (7.21) is a consensus protocol
315 which facilitates the equal contribution of DGs into the reactive power generation

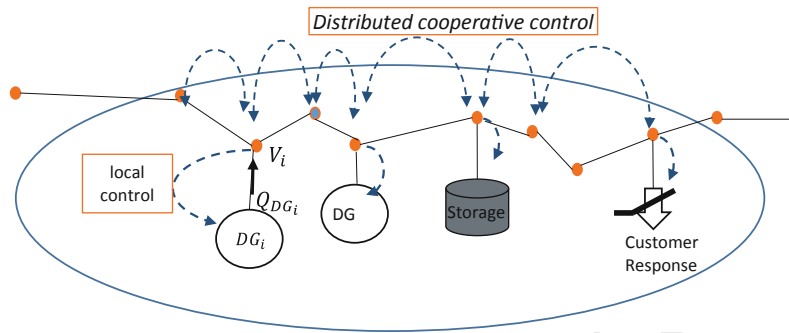


Fig. 7.4 Architecture of cooperative voltage control for distribution network as proposed in [33]

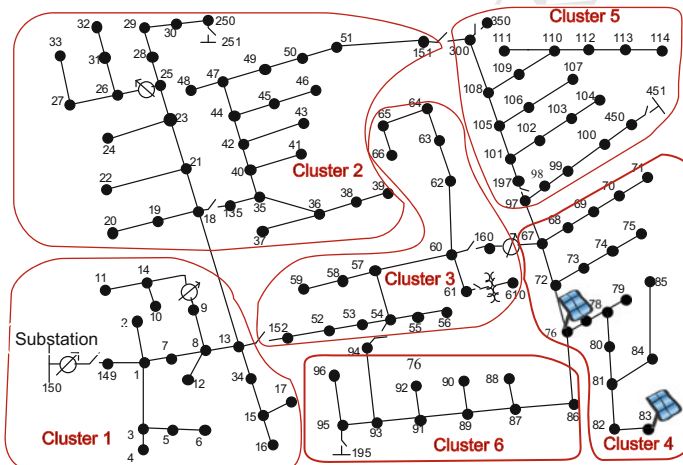


Fig. 7.5 A diagram of IEEE 123 bus system divided into six clusters

316 while the second term corresponds to a (sub)gradient algorithm which minimizes
 317 the objective function in (7.20). Note that a similar strategy can also be applied to
 318 distributed frequency control with DGs as presented in [54].

We evaluate the performance of the cooperative control (7.21) using IEEE 123-bus test system divided into six clusters as shown in Fig. 7.5. The objective is to regulate the bus voltages in cluster 4 with two photovoltaics installed at buses 76 and 83, respectively. The voltage regulation using cooperative control (7.21) is compared with the one using droop control where the droop control gain is manually tuned to achieve the best performance. Figure 7.6 shows the simulation results under both droop control and cooperative control strategies. As can be observed from the figure, droop control strategy results in voltage violations, that is, the voltage of the buses located far away from the substation exceeds the voltage limit of 1.05 p.u. On the other hand, using cooperative control (7.21), the voltage level can be successfully

Fig. 7.6 Comparison of droop control and cooperative control strategies for regulating bus voltages in cluster 4

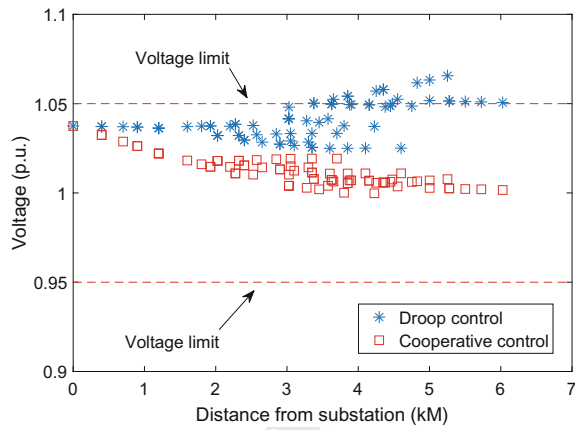
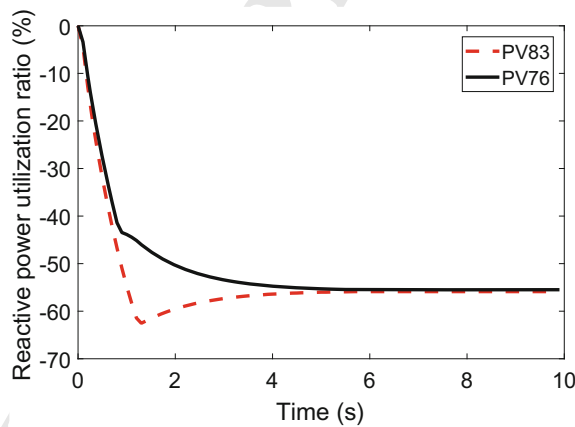


Fig. 7.7 Reactive power fair utilization ratio for the DGs in cluster 4 under cooperative control (7.21)



329 driven close to unity, and thus, the overvoltage problem can be eliminated. In addition,
 330 the cooperative control strategy also yields an equal reactive power fair utilization
 331 ratio for the DGs as shown in Fig. 7.7.

332 7.4.3 High-Level Control Design: Wide-Area Coordination

333 The final step is to design network-level control v_i in (7.7) to ensure the overall
 334 system stability and hence to effectively damp out potential inter-area oscillations.
 335 As discussed in Section 7.3, the design of network-level control depends only on
 336 properties of individual subsystems, in particular their impact coefficient and L_2
 337 parameter quantified by $\{\varepsilon_{ii}, \dots, \varepsilon_{ij}, \dots\}$ and ρ_i , respectively. Similar to (7.15), the
 338 wide-area control v_i is given by

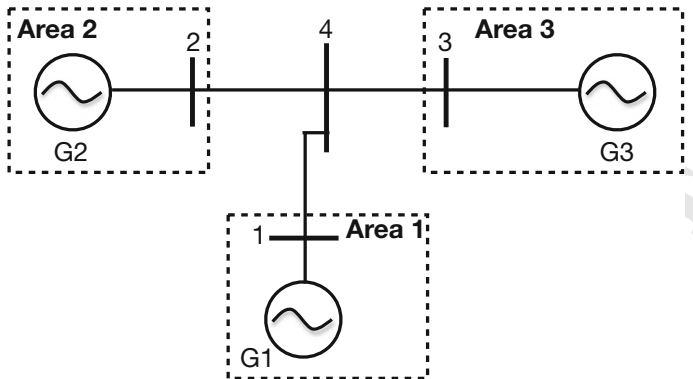


Fig. 7.8 A three-area power system

$$339 \quad v_i = k_{y_i}^w \sum_{j \in \mathcal{N}_i^w} S_{ij}^w (y_j - y_i), \quad (7.22)$$

340 where matrix $S^w = [S_{ij}^w]$ represents the communication network of wide-area control. By choosing control gain $k_{y_i}^w \approx k_w$ and considering storage function $V^w =$
 341 $\sum_i \frac{\gamma_i}{k_w} V_i$, it can be shown by following similar steps as in [44] that system (7.5)
 342 exponentially converges to the desired output consensus provided that control gain
 343 k_w satisfies
 344 k_w satisfies

$$345 \quad -k_w L_w^T \Lambda L_w + (\Gamma_w L_w^T + L_w \Gamma_w) + \frac{\Phi}{k_w} \geq 0,$$

346 where

$$L_w = \text{diag}\{S^w \mathbb{1}\} - S^w, \quad \Lambda = \text{diag}\{\varepsilon_{ii}\}, \quad \Gamma_w = \text{diag}\{\gamma_i\}, \quad \Phi = \text{diag}\{\phi_i\},$$

$$347 \quad \phi_i = \gamma_i \rho_i - \sum_j \gamma_j \varepsilon_{ji}.$$

348 The proposed wide-area control is evaluated using a three-area power system
 349 as illustrated in Fig. 7.8. The simulation time is set to 60s where at $t = 0.0$ s, a
 350 speed disturbance $\Delta = 0.01$ p.u. is added to the system. The wide-area control using
 351 cooperative control (7.22) is compared with the one using traditional control with
 352 typical design (constant gain). The simulation results of power angle for generator 3
 353 for both control strategies are shown in Fig. 7.9. Even though the overall system is
 354 stable under both control strategies, it can be observed from the simulation results that
 355 by using the proposed cooperative control strategy, mitigation of the low-frequency
 356 oscillation (i.e., inter-area oscillation) is considerably improved in comparison to the
 357 oscillation under traditional control with constant gain. Note that similar results can
 358 also be observed for the other two generators in the power system.

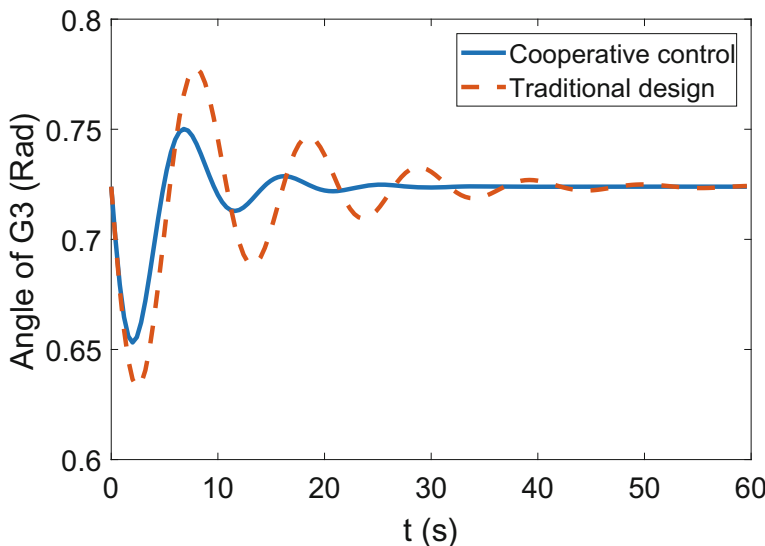


Fig. 7.9 Comparison of power angle for generator 3 under both cooperative wide-area control and traditional control strategies

359 7.5 Analysis of Human–Machine Interaction

360 Human interactions with the physical systems through the cyber components is a cen-
361 tral aspect of cyber-physical-human systems. During the interactions, human may
362 act as an operator such as in teleoperation [24] or semiautonomous robot control sys-
363 tems [3] in general. On the other hand, human may also perform as players or agents
364 in multi-agent systems as can be observed in electricity market [39]. Therefore, it is
365 important to formally and rigorously analyze the human–machine interactions (i.e.,
366 human-in-the-loop control systems) in order to ensure the stability of the intercon-
367 nected systems.

368 Dissipativity theory has been used to model the human decision-making and action
369 in human–machine interactions due to its effectiveness in dealing with the largely
370 unknown human dynamics and its modular design. For example, dissipativity-based
371 modeling is developed and validated in [24] to model human arm endpoint charac-
372 teristics in a human-teleoperated system. In addition, human–machine interactions
373 in semiautonomous robotic swarm is modeled and analyzed in [3] using the concept
374 of passivity-short systems. In particular, it is theoretically shown and experimentally
375 validated that human-operator modeled in [35] can be assumed to be a passivity-
376 short system.

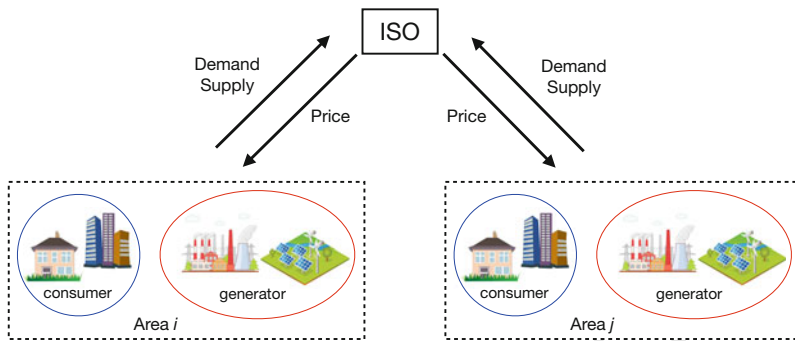


Fig. 7.10 Electricity market consisting of multiple areas

377 7.5.1 Human–Machine Interaction in Electricity Market

378 We focus on human as players or agents in multi-agent systems. As an example, we
 379 consider an electricity market consisting of multiple areas. In the i -th area, there are
 380 set of consumers, generators, and an independent system operator (ISO) engaged
 381 in electricity market trading. Specifically, the consumers and generators decide the
 382 amount of demand and power supply and the ISO uses the information to update
 383 the electricity price in each area as illustrated in Fig. 7.10. The goal is to maximize
 384 the profit of each market participant while balancing the supply and demand. The
 385 problem can be formulated as the following social welfare maximization problem:

$$\begin{aligned}
 & \underset{P_L, P_G}{\text{maximize}} \quad W(P_L, P_G) \\
 & \text{subject to} \quad P_L = P_G, \\
 & \quad \text{linear equality and inequality constraints,}
 \end{aligned} \tag{7.23}$$

386 where W is the social welfare function which depends on the utility function (i.e.,
 387 financial satisfaction) of both the consumers and generators, P_L, P_G are stacks of
 388 total electricity demand and supply in each area, respectively. Note that the solution
 389 to (7.23) may serve as the operational decision r_i in (7.1), see Fig. 7.2. The inequality
 390 constraints in (7.23) include upper and lower bounds on demand and supply. If the
 391 utility function of consumer and generator are strictly concave and convex functions,
 392 respectively, then optimization (7.23) has a unique solution. The convergence analy-
 393 sis of market trading to the solution of (7.23) can be viewed as stability analysis of the
 394 interconnected system of consumers, generators, and ISO as illustrated in Fig. 7.11.
 395 In particular, dynamics of consumer demand, generator supply decisions and ISO
 396 price updating in Fig. 7.11 can be obtained by applying dual decomposition to the
 397 dual problem of (7.23) where its Lagrange multiplier represents the (electricity)
 398 price [38]. When the power demand curve representing input–output static mapping
 399 between (positive) price and demand in electricity market is given in Fig. 7.12a, it
 400 is shown in [39] that each block's dynamics in Fig. 7.11 is (strictly) passive, and as

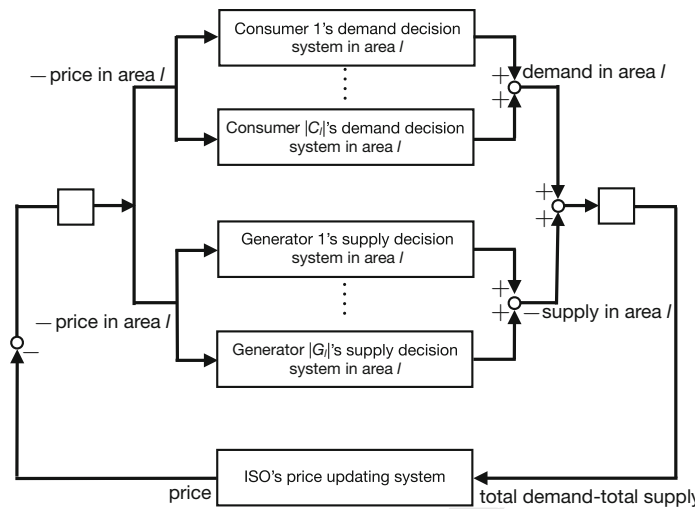


Fig. 7.11 Electricity market trading system in area l viewed as an interconnected system consisting of consumers, generators, and ISO

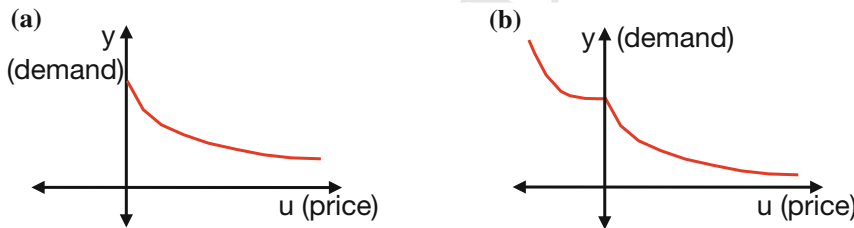


Fig. 7.12 Power demand curve with **a** normal (positive) price; **b** negative price

402 a result, the interconnected system is also passive and hence stable. This means that
 403 the market trading system will converge to the optimal solution of (7.23).

404 However, the price in electricity market is not always positive especially when
 405 the number of renewable energy sources feeding into the power grid increases. For
 406 example, when high and inflexible power generation simultaneously appears and
 407 followed by low electricity demand, power prices may fall below zero (i.e., negative
 408 price) as can be often observed in Germany during public holidays such as Christmas.
 409 This means that power suppliers have to pay their customers to buy electric energy.
 410 The power demand curve when taking into account the negative price can be illus-
 411 trated in Fig. 7.12b. Comparing the figure with input–output diagram in Fig. 7.3a,
 412 it is obvious that dynamics of consumer demand decision system in Fig. 7.11 is
 413 not passive. It is shown in [38] that under power demand curve given in Fig. 7.12b,
 414 dynamics of consumer demand and generator supply decision systems in Fig. 7.11
 415 are passivity-short as can be observed by comparing Figs. 7.3c and 7.12b. As a result,
 416 stability of the electricity market, i.e., interconnected system can still be guaranteed.

417 The discussions above focus on consumer demand decision dynamics derived
 418 from the (static) optimization problem (7.23). Another important issue is the analy-
 419 sis of human decision-making dynamics, that is, how the human responds (in terms
 420 of electricity demand) to the price change with main application to demand response
 421 (e.g., dynamic electricity pricing). There have been some efforts in dynamic modeling
 422 of price-responsive demand in electricity market using real data. For example, empiri-
 423 cal study in [1] using data acquired at ERCOT suggests that (i) demand response
 424 during normal and peak price periods may have qualitatively different behavior, and
 425 (ii) there is a demand response delay on a high price surge. From the empirical
 426 study, we can initially observe that the dynamics of price-responsive demand is not
 427 a passive system due to the delay of the response. Further analysis is still required to
 428 investigate whether the dynamics exhibit passivity-short properties.

429 7.5.2 *Transactive Control*

430 The above example on electricity (competitive) market is a special case of *transactive*
 431 *control*. Transactive control is a new type of framework to coordinate a large number
 432 of distributed generations/loads by combining concepts from microeconomic theory
 433 and control theory [32]. Transactive control extends the concept of demand response
 434 to both the demand and supply sides whose objective is to balance via incentives
 435 (pricing) the supply and demand autonomously, in real-time and a decentralized
 436 manner [46]. In comparison to demand response such as price-responsive control
 437 and direct load control, transactive control preserves customer privacy and has more
 438 predictable and reliable aggregated load response. The potential of transactive control
 439 framework, in particular transactive energy system, has been demonstrated through
 440 several demonstration projects such as the Olympic Peninsula Demonstration [20]
 441 and AEP gridSMART demonstration [53]. Moreover, transactive control framework
 442 has been applied to manage distributed energy resources for different purposes such
 443 as congestion and voltage management [25, 26], providing spinning reserves [52],
 444 and residential energy management [37].

445 Broadly speaking, transactive control framework can be modeled using four key
 446 elements as proposed in [32]: payoff functions, control decisions, information, and
 447 solution concept. Consider a system consisting of $(n + 1)$ agents, that is one coordi-
 448 nator (agent 0) and n distributed energy resources (DERs) where each DER can
 449 communicate with each other and also with the coordinator to perform local decision-
 450 making. Local objective of both coordinator and DERs is represented by a payoff
 451 function U_i which depends on price μ_i and energy consumption p_i . Each DER aims
 452 at maximizing its own payoff function formulated as

$$453 \begin{aligned} & \text{maximize} \quad U_i(\mu_i, p_i; \theta_i) \\ & \text{subject to} \quad h_i(p_i; \theta_i) \leq 0, \end{aligned}$$



454 where θ_i denotes private information of the agent such as preference and local
 455 constraints. Similarly, the coordinator aims to solve the following optimization problem:

456

$$\begin{aligned} & \text{maximize} && U_0(\mu, p; \theta) \\ & \text{subject to} && g(p, \mu; \theta) \leq 0; \quad h_i(p_i; \theta_i) \leq 0, \end{aligned}$$

457 where $p = [p_1, \dots, p_n]^T$, $\mu = [\mu_1, \dots, \mu_n]^T$ and $\theta = [\theta_1, \dots, \theta_n]^T$. Note that the
 458 payoff function of coordinator depends on prices and consumption of all DERs.
 459 Moreover, the coordinator also has a global constraint such as power flow constraint
 460 in the whole network. Next, to optimize the payoff functions, control decision are
 461 defined for each agent denoted by $\pi_i \in \Pi_i$ where Π_i is the feasible control deci-
 462 sion of agent i . For example, by taking $\pi_0 = \mu$ and $\pi_i = p_i$ the payoff functions
 463 become $U_i(\pi_i, \pi_0; \theta_i)$ and $U_0(\pi_0, \pi_1, \dots, \pi_n; \theta)$ which yields a coupling between
 464 decisions of DERs and coordinator. Another important element in transactive con-
 465 trol is information set available to each agent, denoted by Γ_i . Information set Γ_i
 466 consists of private information and information of control decision of each agent.
 467 Finally, information on control decisions provides a sequence of decision for the
 468 agents resulting in a multilevel decision problem. Within each layer, if the payoff
 469 function of each agent does not depend on decisions of other players then the solution
 470 is simply equal to the optimal solution to the standard optimization problem. On the
 471 other hand, if the payoff functions of each agent depends on the other agents, then
 472 we have a game problem whose solution corresponds to the game equilibrium. Two
 473 basic solution concepts to a game problem are Nash equilibrium (that is a collection
 474 of decisions from which no agent wants to deviate given that others stick to the equi-
 475 librium decision) and dominant strategy equilibrium (that is each agent will stick to
 476 the equilibrium strategy no matter what decisions other players make).

477 The four elements described above dictate the class of transactive problems (type
 478 of games) under consideration. For example, if the agent's payoff function is quasi-
 479 linear w.r.t. price and the coordinator's objective is to minimize the overall operational
 480 cost while satisfying some constraints, then we have a social maximization problem
 481 described in the previous subsection. On the other hand, if the payoff function is not
 482 quasi-linear and the coordinator's objective is different from maximizing the social
 483 welfare, we then have a Stackelberg game whose equilibrium computation is very
 484 challenging [6, 47, 49, 50].

485 Research challenges in transactive control include investigating price-response
 486 behavior of DERs and ensuring convergence of transaction control. For example,
 487 it is shown in [40] that a simple price strategy may stabilize the power system
 488 operation. Dissipativity theory provides a framework to systematically analyze this
 489 complex system as demonstrated in the previous subsection. Further research need
 490 to be performed to investigate the application of dissipativity theory for analyzing
 491 different transactive control problems.

492 7.6 Role of Real-Time Big Data and Decision-Making

493 The hierarchical control/optimization architecture presented in the previous subsec-
494 tions relies on real-time big data. Rapid development of sensor, wireless transmission,
495 network communication technologies, smart devices, and cloud computing makes
496 it possible to collect large amounts of data in real time. To illustrate further this
497 point, let us take a smart grid as an example. The main data source in smart grid is
498 the advanced metering infrastructure (AMI) which deploys a large number of smart
499 meters at the end-user side and collects, e.g., customers' electricity consumption
500 data every 15 min [28, 56]. It is estimated that the amount of data collected by AMI
501 will increase from 24 million a year to 220 million per day for a large utility com-
502 pany [56]. Moreover, the volume of data collected every 15 mins in a distribution
503 network using 1 million devices will surge up to 2920 Tb [31]. In addition to AMI,
504 PMUs are able to produce direct time-stamped voltage/current magnitudes and phase
505 angle with sampling rate 30–60 samples per second, which is much faster than the
506 data collection in Supervisory Control and Data Acquisition (SCADA) system [7].
507 As an illustration, the amount of data per day generated by 100 PMUs with 20 mea-
508 surements and at the sampling rate of 60 Hz is equal to 100 GB [30]. Other sources of
509 big data in smart grid include weather data, mobile data, thermal sensing data, energy
510 database, electric vehicle data, transmission line sensor, and dynamic pricing [56].

511 The increase of uncertainty (e.g., due to the high renewable energy penetration)
512 and tight interconnection between and within the layers calls for real-time process-
513 ing and decision-making. To this end, big data can be utilized for developing novel
514 real-time learning, optimization, and decision-making (control) algorithms for cyber-
515 physical-human systems as illustrated in the previous sections. For example, big data
516 has many applications in the operation of smart grid [48]. A new algorithms using
517 PMU data is proposed in [8] to accelerate the state estimation process. Moreover, a
518 PMU based robust estimation method is presented in [55] to eliminate unwanted per-
519 turbed data and thus increases the robustness of state estimation algorithm. Big data
520 can also be used for fault detection and classification in micro-grid leading to a much
521 better performance compared to model-based approach [36]. AMI and other sensors
522 provide opportunity to realize line impedance calibration (i.e., parameters) for distri-
523 bution power system which was not possible previously [41]. Weather data can also
524 be used for predicting the power generation of renewable energy sources such as wind
525 turbines which further can be utilized for voltage control and demand response [19].
526 Furthermore, with the exponentially increasing number of PMUs deployed, and the
527 resulting explosion in data volume, wide-area measurement systems (WAMS) tech-
528 nology as the key to guaranteeing stability, reliability, situational awareness, state
529 estimation, and control of next-generation power systems is bound to transcend from
530 centralized to a distributed architecture within the next few years. Motivated by this
531 fact, a distributed optimization based learning algorithm is proposed in [10] for one
532 of the most critical wide-area monitoring applications—namely, estimation of mode
533 shapes for inter-area oscillation modes.

534 The exposure to external network such as Internet comes at a price of data security
535 and privacy [29, 34]. Cyber incidents or network intrusion may cause physical dam-
536 age to the physical system due to the tight coupling between the physical system and
537 the cyber-layer. Unfortunately, traditional security solutions in the ICT (information
538 and communications technology) domain are not sufficient to ensure security and
539 resilience of the network since they do not take into account the physical attacks
540 through direct interaction with the components in physical systems. For example, by
541 placing a shunt around a meter the integrity of a meter can be violated without the
542 need of breaking the cybersecurity countermeasure. They may also introduce adverse
543 effects on the operation of CPS. For example, while cryptography can enhance the
544 confidentiality of data flows, it may result in unacceptable time latency and degrade
545 the performance of time-critical functionalities in CPS. Moreover, coordinated net-
546 work attacks by sophisticated adversaries undermine standard residual based detec-
547 tion schemes. It is discussed in [13, 14] that control theoretic framework together
548 with recent advancement in cloud computing and network management (e.g., soft-
549 ware defined networking) show promises in ensuring the resilient operation of CPS
550 against (coordinated and intelligent) cyberattacks.

551 7.7 Conclusion

552 The chapter presents a scalable and modular control-theoretical framework to model,
553 analyze, optimize, and control cyber-physical-human systems. It is shown that effi-
554 cient computational algorithms can be applied hierarchically to operate and optimize
555 cyber-physical-human systems, first individually to quantify the dynamic behavior of
556 every agent, then locally to describe the local interactions of neighboring agents, and
557 finally to the overall system. All the three control levels deal with real-time big data,
558 and the hierarchical structure makes the overall optimization and control problem
559 scalable and solvable. In particular, we present and highlight two main tools whose
560 combination shows a great promise to optimize and control such tightly intercon-
561 nected system. The first tool is the concept of dissipativity theory which is a useful
562 way of quantifying input-output properties of dynamical systems and whose com-
563 positional property makes it a powerful tool to analyze and control CPS. The second
564 tool is cooperative control which allows the designer to develop a scalable and robust
565 optimization and control algorithms. Application to power system is investigated as
566 an illustrative example.

567 **Acknowledgements** This work is supported in part by U.S. Department of Transportation (award
568 DTTR13GUTC51), by U.S. National Science Foundation (grant ECCS-1308928), by US Depart-
569 ment of Energy (awards DE-EE0006340, DE-EE0007327, and DE-EE0007998), by L-3 Commu-
570 nication Coleman Aerospace (contract 11013I2034), by Texas Instruments' awards, and by Leidos
571 (contract P010161530).

572 References

1. An, J., Kumar, P., Xie, L.: On transfer function modeling of price responsive demand: an empirical study. In: IEEE Power and Energy Society General Meeting, pp. 1–5 (2015)
2. Antsaklis, P.J., Goodwine, B., Gupta, V., McCourt, M.J., Wang, Y., Wu, P., Xia, M., Yu, H., Zhu, F.: Control of cyberphysical systems using passivity and dissipativity based methods. *Eur. J. Control.* **19**(5), 379–388 (2013)
3. Atman, M.W.S., Hatanaka, T., Qu, Z., Chopra, N., Yamauchi, J., Fujita, M.: Motion synchronization for semi-autonomous robotic swarm with a passivity-short human operator. *Int. J. Intell. Robot. Appl.* **2**(2), 235–251 (2018)
4. Baheti, R., Gill, H.: Cyber-physical systems. *Impact Control Technol.* **12**(1), 161–166 (2011)
5. Cassandras, C.G.: Smart cities as cyber-physical social systems. *Engineering* **2**(2), 156–158 (2016)
6. Colson, B., Marcotte, P., Savard, G.: An overview of bilevel optimization. *Ann. Oper. Res.* **153**(1), 235–256 (2007)
7. DOE: Advancement of synchrophasor technology in ARRA projects. https://www.smartgrid.gov/recovery_act/program_publications.html
8. Göl, M., Abur, A.: A fast decoupled state estimator for systems measured by PMUs. *IEEE Trans. Power Syst.* **30**(5), 2766–2771 (2015)
9. Gusrialdi, A.: Performance-oriented communication topology design for distributed control of interconnected systems. *Math. Control Signals Syst.* **25**(4), 559–585 (2013)
10. Gusrialdi, A., Chakrabortty, A., Qu, Z.: Distributed learning of mode shapes in power system models. In: IEEE Conference on Decision and Control, pp. 4002–4007 (2018)
11. Gusrialdi, A., Qu, Z.: Growing connected networks under privacy constraint: achieving trade-off between performance and security. In: IEEE Conference on Decision and Control, pp. 312–317. IEEE (2015)
12. Gusrialdi, A., Qu, Z.: Distributed estimation of all the eigenvalues and eigenvectors of matrices associated with strongly connected digraphs. *IEEE Control Syst. Lett.* **1**(2), 328–333 (2017)
13. Gusrialdi, A., Qu, Z.: Smart grid security: attacks and defenses. In: Stoustrup, J., Annaswamy, A., Chakrabortty, A., Qu, Z. (eds.) *Smart Grid Control: An Overview and Research Opportunities*, pp. 199–223. Springer (2018)
14. Gusrialdi, A., Qu, Z.: Towards resilient operation of smart grid. In: Stoustrup, J., Annaswamy, A., Chakrabortty, A., Qu, Z. (eds.) *Smart Grid Control: An Overview and Research Opportunities*, pp. 275–288. Springer (2018)
15. Gusrialdi, A., Qu, Z., Hirche, S.: Distributed link removal using local estimation of network topology. *IEEE Trans. Netw. Sci. Eng.* (2018)
16. Gusrialdi, A., Qu, Z., Simaan, M.A.: Distributed scheduling and cooperative control for charging of electric vehicles at highway service stations. *IEEE Trans. Intell. Transp. Syst.* **18**(10), 2713–2727 (2017)
17. Gusrialdi, A., Qu, Z., Simaan, M.A.: Competitive interaction design of cooperative systems against attacks. *IEEE Trans. Autom. Control* **63**(9), 3159–3166 (2018)
18. Gusrialdi, A., Yu, C.: Exploiting the use of information to improve coverage performance of robotic sensor networks. *IET Control Theory Appl.* **8**(13), 1270–1283 (2014)
19. Hagh, H.V., Qu, Z.: A Kernel-based predictive model of EV capacity for distributed voltage control and demand response. *IEEE Trans. Smart Grid* **9**(4), 3180–3190 (2018)
20. Hammerstrom, D.J., Ambrosio, R., Carlton, T.A., DeSteele, J.G., Horst, G.R., Kajfaz, R., Kiesling, L.L., Michie, P., Pratt, R.G., Yao, M., et al.: Pacific northwest gridwise? Testbed demonstration projects; Part I. Olympic Peninsula Project. Technical report, Pacific Northwest National Lab. (PNNL), Richland, WA (United States) (2008)
21. Harvey, R., Qu, Z.: Cooperative control and networked operation of passivity-short systems. In: *Control of Complex Systems*, pp. 499–518. Elsevier (2016)
22. Harvey, R., Xu, Y., Qu, Z., Namerikawa, T.: Dissipativity-based design of local and wide-area DER controls for large-scale power systems with high penetration of renewables. In: IEEE Conference on Control Technology and Applications, pp. 2180–2187 (2017)

625 23. Hill, D., Moylan, P.: The stability of nonlinear dissipative systems. *IEEE Trans. Autom. Control*
626 **21**(5), 708–711 (1976)

627 24. Hirche, S., Buss, M.: Human-oriented control for haptic teleoperation. *Proc. IEEE* **100**(3),
628 623–647 (2012)

629 25. Hu, J., You, S., Lind, M., Ostergaard, J.: Coordinated charging of electric vehicles for congestion
630 prevention in the distribution grid. *IEEE Trans. Smart Grid* **5**(2), 703–711 (2014)

631 26. Ipakchi, A.: Demand side and distributed resource management—a transactive solution. In: IEEE
632 Power and Energy Society General Meeting, pp. 1–8 (2011)

633 27. Joo, Y., Harvey, R., Qu, Z.: Cooperative control of heterogeneous multi-agent systems in a
634 sampled-data setting. In: IEEE Conference on Decision and Control, pp. 2683–2688 (2016)

635 28. Karnouskos, S., Terzidis, O., Karnouskos, P.: An advanced metering infrastructure for future
636 energy networks. In: New Technologies, Mobility and Security, pp. 597–606. Springer (2007)

637 29. Khurana, H., Hadley, M., Lu, N., Frincke, D.A.: Smart-grid security issues. *IEEE Secur. Priv.*
638 **8**(1) (2010)

639 30. Klump, R., Agarwal, P., Tate, J.E., Khurana, H.: Lossless compression of synchronized phasor
640 measurements. In: IEEE Power and Energy Society General Meeting, pp. 1–7 (2010)

641 31. Lavastorm: Big data, analytics, and energy consumption. <http://www.lavastorm.com/blog/2012/04/09/big-data-analytics-and-energy-consumption/>

642 32. Lian, J., Zhang, W., Sun, Y., Marinovici, L.D., Kalsi, K., Widergren, S.E.: Transactive system:
643 Part I: Theoretical underpinnings of payoff functions, control decisions, information privacy,
644 and solution concepts. Technical report, Pacific Northwest National Lab. (PNNL), Richland,
645 WA (United States) (2018)

646 33. Maknounejad, A., Qu, Z.: Realizing unified microgrid voltage profile and loss minimization:
647 a cooperative distributed optimization and control approach. *IEEE Trans. Smart Grid* **5**(4),
648 1621–1630 (2014)

649 34. McDaniel, P., McLaughlin, S.: Security and privacy challenges in the smart grid. *IEEE Secur.*
650 *Priv.* **3**, 75–77 (2009)

651 35. McRuer, D.: Human dynamics in man-machine systems. *Automatica* **16**(3), 237–253 (1980)

652 36. Mishra, D.P., Samantaray, S.R., Joos, G.: A combined wavelet and data-mining based intelligent
653 protection scheme for microgrid. *IEEE Trans. Smart Grid* **7**(5), 2295–2304 (2016)

654 37. Moradzadeh, B., Tomsovic, K.: Two-stage residential energy management considering network
655 operational constraints. *IEEE Trans. Smart Grid* **4**(4), 2339–2346 (2013)

656 38. Muto, K., Namerikawa, T., Qu, Z.: Passivity-short-based stability analysis on electricity market
657 trading system considering negative price. In: IEEE Conference on Control Technology and
658 Applications, pp. 418–423 (2018)

659 39. Okawa, Y., Namerikawa, T., Qu, Z.: Passivity-based stability analysis of dynamic electricity
660 pricing with power flow. In: IEEE Conference on Decision and Control, pp. 813–818 (2017)

661 40. Pentland, A.: Economics: simple market models fail the test. *Nature* **525**(7568), 190 (2015)

662 41. Peppanen, J., Reno, M.J., Broderick, R.J., Grijalva, S.: Distribution system model calibration
663 with big data from AMI and PV inverters. *IEEE Trans. Smart Grid* **7**(5), 2497–2506 (2016)

664 42. Qu, Z.: Cooperative Control of Dynamical Systems. Springer, London (2009)

665 43. Qu, Z., Simaan, M.: An analytic solution to the optimal design of information structure and
666 cooperative control in networked systems. In: IEEE Conference on Decision and Control, pp.
667 4015–4022 (2012)

668 44. Qu, Z., Simaan, M.A.: Modularized design for cooperative control and plug-and-play operation
669 of networked heterogeneous systems. *Automatica* **50**(9), 2405–2414 (2014)

670 45. Sepulchre, R., Jankovic, M., Kokotovic, P.: Constructive Nonlinear Control. Springer, London
671 (1997)

672 46. Sijie, C., Chen-Ching, L.: From demand response to transactive energy: state of the art. *J. Mod.*
673 *Power Syst. Clean Energy* **5**(1), 10–19 (2017)

674 47. Soliman, H.M., Leon-Garcia, A.: Game-theoretic demand-side management with storage
675 devices for the future smart grid. *IEEE Trans. Smart Grid* **5**(3), 1475–1485 (2014)

676 48. Tu, C., He, X., Shuai, Z., Jiang, F.: Big data issues in smart grid—a review. *Renew. Sustain.*
677 *Energy Rev.* **79**, 1099–1107 (2017)



679 49. Tushar, W., Saad, W., Poor, H.V., Smith, D.B.: Economics of electric vehicle charging: a game
680 theoretic approach. *IEEE Trans. Smart Grid* **3**(4), 1767–1778 (2012)

681 50. Tushar, W., Zhang, J.A., Smith, D.B., Poor, H.V., Thiébaux, S.: Prioritizing consumers in smart
682 grid: a game theoretic approach. *IEEE Trans. Smart Grid* **5**(3), 1429–1438 (2014)

683 51. VanAntwerp, J.G., Braatz, R.D.: A tutorial on linear and bilinear matrix inequalities. *J. Process
684 Control* **10**(4), 363–385 (2000)

685 52. Weckx, S., D’hulst, R., Driesen, J.: Primary and secondary frequency support by a multi-agent
686 demand control system. *IEEE Trans. Power Syst.* **30**(3), 1394–1404 (2015)

687 53. Widergren, S.E., Subbarao, K., Fuller, J.C., Chassin, D.P., Soman, A., Marinovici, M.C., Ham-
688 merstrom, J.L.: AEP Ohio gridSMART demonstration project real-time pricing demonstration
689 analysis. *PNNL Rep.* **23192** (2014)

690 54. Xin, H., Qu, Z., Seuss, J., Maknouninejad, A.: A self-organizing strategy for power flow control
691 of photovoltaic generators in a distribution network. *IEEE Trans. Power Syst.* **26**(3), 1462–1473
692 (2011)

693 55. Zhao, J., Zhang, G., Das, K., Korres, G.N., Manousakis, N.M., Sinha, A.K., He, Z.: Power
694 system real-time monitoring by using PMU-based robust state estimation method. *IEEE Trans.
695 Smart Grid* **7**(1), 300–309 (2016)

696 56. Zhou, K., Fu, C., Yang, S.: Big data driven smart energy management: from big data to big
697 insights. *Renew. Sustain. Energy Rev.* **56**, 215–225 (2016)

Author Queries

Chapter 7

Query Refs.	Details Required	Author's response
AQ1	Please note that mismatch has been found between author pdf and tex, we followed tex source. Kindly check and confirm.	
AQ2	Please check the edit made in the chapter and running titles.	
AQ3	Please check if the edit made in the sentence 'While technological advances...' conveys the intended meaning.	

MARKED PROOF

Please correct and return this set

Please use the proof correction marks shown below for all alterations and corrections. If you wish to return your proof by fax you should ensure that all amendments are written clearly in dark ink and are made well within the page margins.

Instruction to printer	Textual mark	Marginal mark
Leave unchanged	... under matter to remain	✓
Insert in text the matter indicated in the margin	↪	New matter followed by ↪ or ↪ ^②
Delete	/ through single character, rule or underline ———— through all characters to be deleted	⊖ or ⊖ ^②
Substitute character or substitute part of one or more word(s)	/ through letter or ———— through characters	new character / or new characters /
Change to italics	— under matter to be changed	←
Change to capitals	≡ under matter to be changed	≡
Change to small capitals	— under matter to be changed	—
Change to bold type	~ under matter to be changed	~
Change to bold italic	~~ under matter to be changed	~~
Change to lower case	Encircle matter to be changed	≡
Change italic to upright type	(As above)	+
Change bold to non-bold type	(As above)	—
Insert 'superior' character	/ through character or ↪ where required	Y or X under character e.g. ³ or ³
Insert 'inferior' character	(As above)	↪ over character e.g. ²
Insert full stop	(As above)	○
Insert comma	(As above)	,
Insert single quotation marks	(As above)	Y or X and/or Y or X
Insert double quotation marks	(As above)	“ or ” and/or “ or ”
Insert hyphen	(As above)	—
Start new paragraph	—	—
No new paragraph	≈	≈
Transpose	—	—
Close up	linking () characters	()
Insert or substitute space between characters or words	/ through character or ↪ where required	Y
Reduce space between characters or words	between characters or words affected	↑